SFB 805 Demonstrator

Technical Report on operation, numerical simulation and experimental analysis of MAFDS

Darmstadt, 30. November 2017

Author: Mallapur, S.

TECHNISCHE
UNIVERSITÄT
DARMSTADT

Contents

1 Introduction to Experimental MAFDS

This report describes the experimental test rig of an academic suspension strut system which is referred as the modular active spring-damper system (German acronym MAFDS). MAFDS is developed under the framework of German Collaborative Research Center SFB 805 at the Technische Universität Darmstadt. The concept of MAFDS is registered as a Patent DE 10 2014 106 858.A1 "Load transferring device" [1]. The MAFDS along with its test rig is referred as SFB 805 Demonstrator.

1.1 MAFDS

As illustrated in Fig. 1.1, the MAFDS serves as an academic demonstrator to investigate the different methods and technologies to control uncertainty in all development stages such as the conceptual phase, design and optimization phase, production and assembly phase as well as the final operational phase. Uncertainty is investigated especially for MAFDS's main operating function and purpose: sustain stability, well balanced load distribution and ability to attenuate vibrations. Passive, semi-active and active technology approaches for stability, load distribution

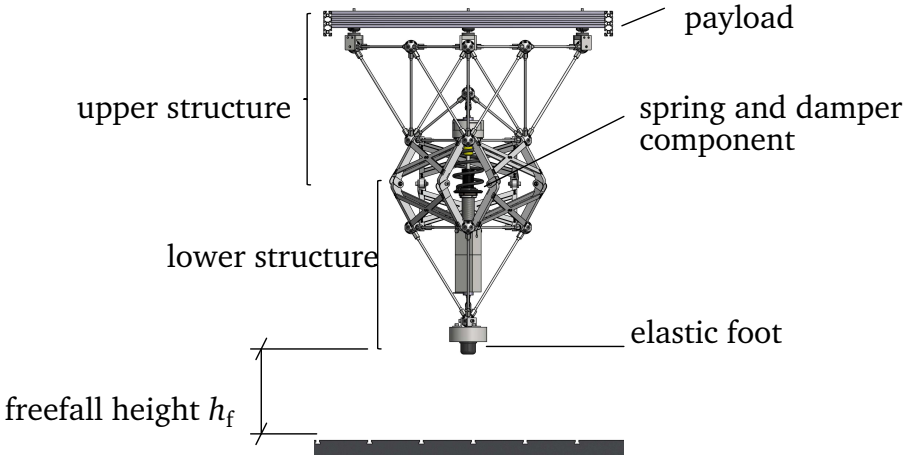

Figure 1.1: CAD illustration of a suspension strut (MAFDS)

and vibration control to compensate uncertainty in the main functions mentioned above are integrated in a modular way within SFB 805, [3], [4], [5], [6]. MAFDS has similar dynamic requirements of a typical suspension strut such as an aircraft landing gear. However it is not designed to be used as a substitute to an existing aircraft landing gear. Rather, the MAFDS is an academic example to study the uncertainty in the dynamic responses of suspension strut systems in a general way as explained above. For further details on the passive, semi-active and active components of the MAFDS, please refer [2].

1.2 Experimental input and output variables of MAFDS

The uncertainty in the experimental dynamic response of the MAFDS is quantified and evaluated for four different loading conditions, refer Fig. 1.2. In the first case a), static loading of MAFDS

is accomplished by placing additional payload on the upper structure. The static payloads can be varied in steps of 5 kg from 0 to 200 kgs. The second type of loading b) is the drop test that is conducted by raising the MAFDS to a certain drop height h and releasing it thereafter under the influence of the acceleration due to earth's gravity g. In this case, the MAFDS drops down symmetrically. However, in the third scenario c), the MAFDS is released from the drop height h with an inclination angle. This inclination angle is achieved by placing additional displacement blocks in the housing supports of the MAFDS. In the final loading scenario d), the MAFDS is excited with an electrodynamic vibrational shaker. The objective is to simulate the ground excitation of the MAFDS due to a road profile. The intended amplitude and frequency ranges of the road profile are listed in table 1.1. The experimental output variables of the MAFDS that

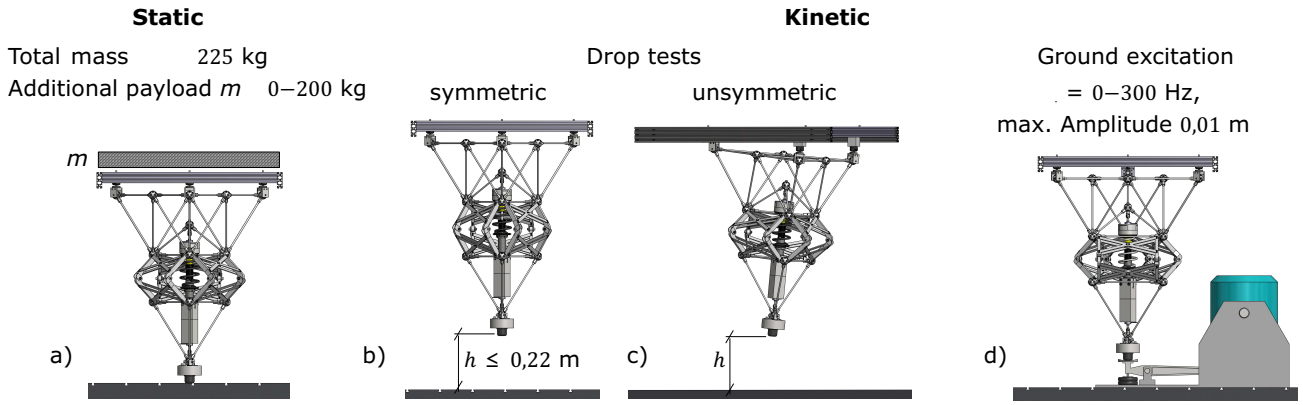

Figure 1.2: CAD illustration of the different loading conditions of the suspension strut (MAFDS)

Table 1.1: Summary of experimental input variables

Input variable	Variation range	Variation resolution	Loading cases
Additional payload	225 - 425 kg	5 kg	cases a) to d)
Drop height	0 - 0.22 m	0.005 m	cases b) and c)
Inclination angle	0 - 6 °	3 °	case c)
Excitation amplitude	0 - 0.01 m	-	case d)
Excitation frequency	0 - 300 Hz	-	case d)

are measured to quantify and evaluate the uncertainty in its dynamic response remains same for all the four loading conditions. Moreover, the same experimental output variables are measured for the passive, semi-active as well as active components of MAFDS. Fig. 1.3 illustrates the location of the output variables that are measures for all the four loading conditions. A list of the measured output variables and the corresponding sensors are described in table 1.2. The forces in the MAFDS are introduced via the housing supports at locations 1-3 and via the elastic foot component at location 6. Axial forces exerted by the spring-damper component are measured at locations 4 and 5 using 1-axial strain gauge force sensors.

As listed in table 1.2, the accelerations are measured at locations 7-9. The relative displacement between the upper and lower truss components are measured using the linear displacement differential transformer LVDT sensors. Moreover, the axial forces and the bending moments in the beam-columns of MAFDS are measured using the strain gauge sensors. These are measured at locations 11-20 in the upper and lower truss components of MAFDS.

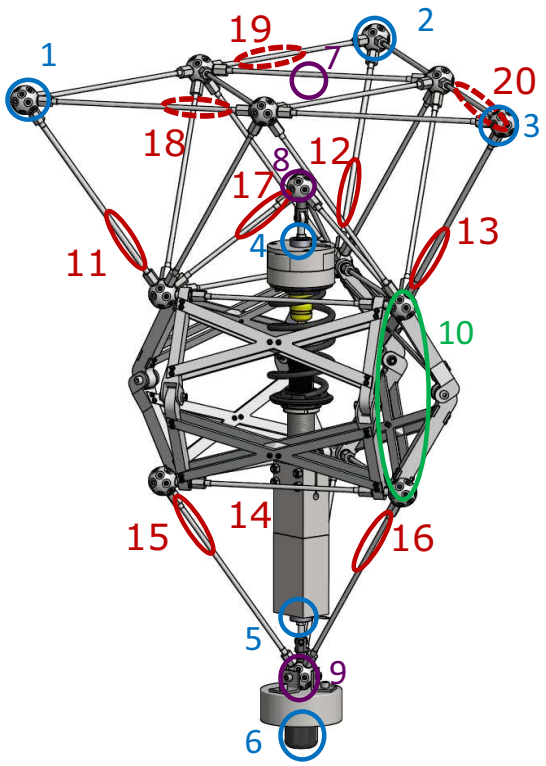

Figure 1.3: CAD illustration of the location of the measured output variables of MAFDS

Table 1.2: Summary of experimental output variables

Output variable	Sensor Location	Nr.	Sensor Type	Channels
Force	Housing support	1-3	3-ax. piezoelectric force sensor	9
	Spring-damper above	4	1-ax. strain gauge force sensor	1
	Spring-damper below	5	1-ax. strain gauge force sensor	1
	Ground impact	6	3-ax. strain gauge force sensor	3
Acceleration	Load frame	7	1-ax. accelerometer	1
	Spring-damper above	8	3-ax. accelerometer	3
	lower payload	9	3-ax. accelerometer	3
Compression	Distance between upper and lower truss	10	LVDT sensor	3
Normal and bending strains	outer beams, upper truss	11-13	strain gauges (3x4)	9
	outer beams, lower truss	14-16	strain gauges (3x4)	9
	1 beam, spring-damper	17	strain gauges (1x4)	3
bending strains	upper beams, upper truss	18-20	strain gauges (3x4)	6
				$\Sigma = 51$

An important application of the measured output variables is to quantify and evaluate the uncertainty in the mathematical modelling of the MAFDS. Mathematical models based on rigid body motion and finite element methods can be utilized for the computation of the output variables of MAFDS, refer [2], [7] and [8] for further details. Model validation techniques

are used to address the problem with the model form uncertainty that exists in the different mathematical models that are used to predict the dynamic response of the MAFDS.

1.3 Test rig of MAFDS

Fig. 1.4 describes the test rig of the MAFDS. The MAFDS is fixed at three points to the load frame 1 by means of three housing supports 2. The hoist frame 3 and the load frame are connected by an electro-pneumatic coupling 4. The hoist and the load frames are fixed to the guide blocks 5 that allow smooth parallel movement of the MAFDS along the guide rails 6. The hoist frame is driven by two servomotors 7 that run synchronously.

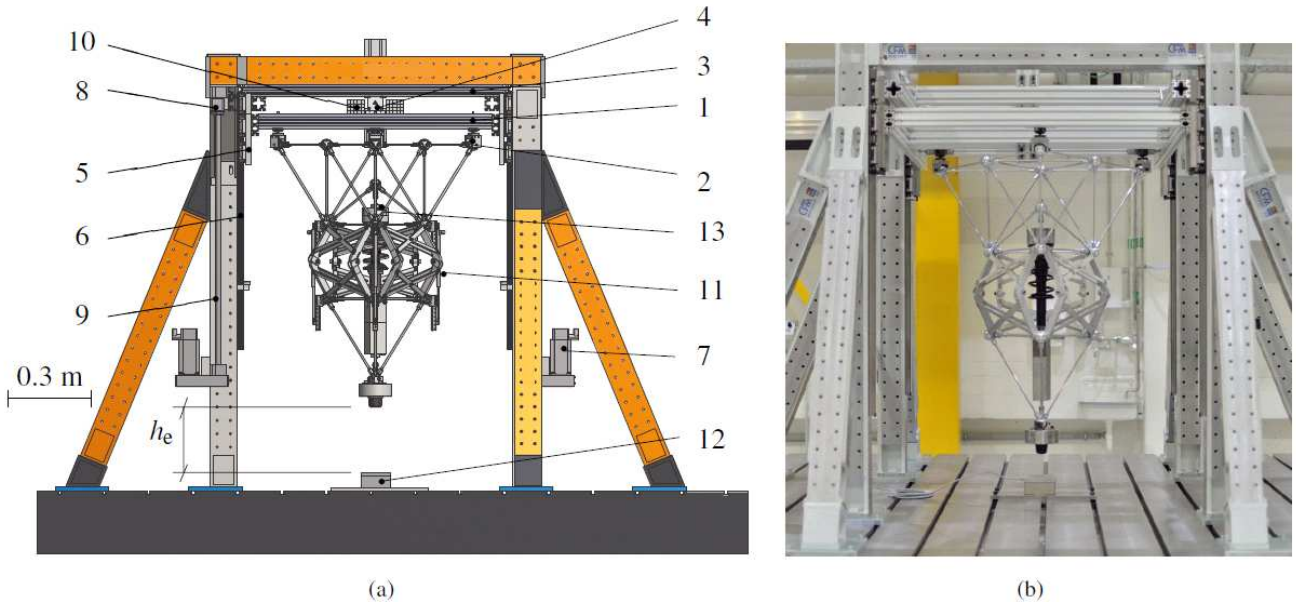

Figure 1.4: (a)CAD illustration and (b) real photo of SFB 805 Demonstrator

Table 1.3: Components of the experimental rig

No.	Component	No.	Component	No.	Component
1	load frame	2	housing support	3	hoist frame
4	electro-pneumatic coupling	5	guide blocks	6	guide rails
7	servomotors	8	ball screw	9	threaded spindle
10	addditional payloads	11	displacement sensor	12	3-axial force sensor
13	1-axial force sensor				

The ball screw 8 converts the rotational motion of the threaded spindle 9, which is powered by the servomotors into the translational parallel movement of the hoist frame. Once lifted to the desired experimental height h, the MAFDS can be released by the pneumatic coupling for a drop test. The maximum experimental drop height of MAFDS is $h_{\max} = 0.22$ m. Additional payloads 10 can be fixed to the load frame, thereby adding static loads to the MAFDS.

2 Operating instructions for conducting the drop tests

As mentioned earlier the SFB 805 Demonstrator consists of the academic example of aircraft landing gear called MAFDS and the test rig. The drop tests of MAFDS are carried out using two computers NBTUD08 and PCTUD33. The laptop NBTUD08 is used to operate the parallel movement of MAFDS along the guide rails as well as its release and recoupling from the hoist frame. Refer section 1.3, Fig. 1.4 and table 1.3 for details about the components of SFB 805 Demonstrator. These activities are controlled by Rexroth controller that is connected to NBTUD08 via a local LAN network. The data acquisition system DAQ used to record the experimental observations of MAFDS is connected to PCTUD33 via a different local LAN network.

The data acquisition system is manufactured and delivered from imc GmbH. The contact person for queries regarding the purchase and enhancement of the DAQ system is **Mr. Thorsten Störr**. For the technical support, the contact person is **Mr. Martin Arndt** with the telephone number +49 6172 59672-40. The documentation for the imc DAQ system can be found under: `O:\Arbeitsgruppen\SFB805\SFB_Demonstrator\1_Dokumentation\6_Datenblaetter\imc`

2.1 Starting SFB 805 Demonstrator

Step 1. The first step is to turn on the power button of the Bosch Rexroth controller. After turning on the controller, the reset button must start blinking, refer Fig. 2.1. In case the controller fails to turn on, open the cabinet and check if the circuit breaker is tripped. Push the circuit breaker up in order to restore the power supply to the controller cabinet. For conducting drop tests, the reset button should not be blinking. Hence, push the blinking reset button to activate the safety and release mechanism of SFB-Demonstrator. In case of emergency, press the safety button in order to disrupt the power supply abruptly.

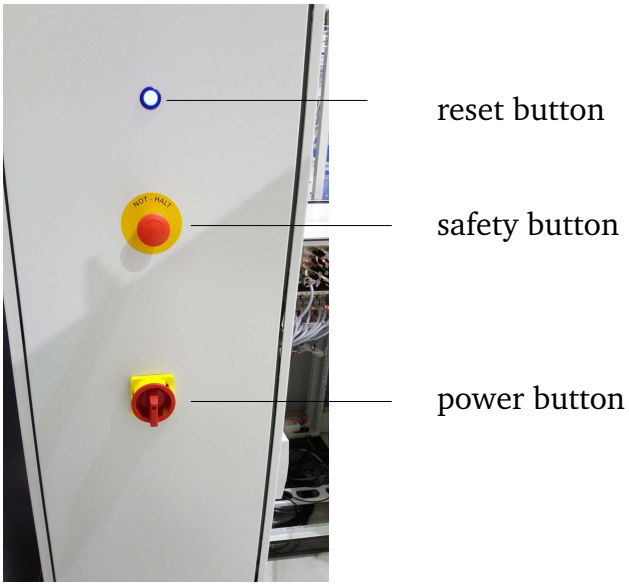

Figure 2.1: Turning on the Bosch Rexroth controller housed in the cabinet

Step 2. Next push the green button to turn the data acquisition DAQ system on. Please wait for

around 30 seconds for the DAQ system to start up. Check the numbering on the measurement modules. It should be numbered from 0 to 9.

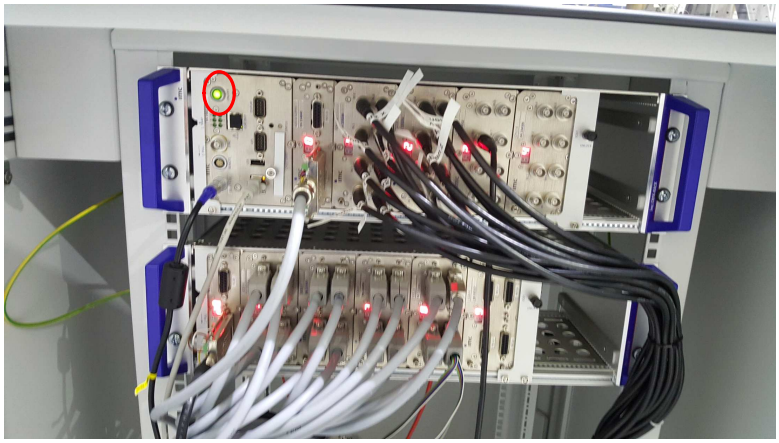

Figure 2.2: Turning the Data acquisition system on

Step 3. Next step is to switch on the Laptop NBTUD08 and the Computer PCTUD33. The Indralogic software to control the parallel movement of the MAFDS along the guide rails and to release the MAFDS from a certain drop height h is installed on the Laptop NBTUD08. Whereas, the imc Studio and imc FAMOS Professional 7.1 softwares to operate the data acquisition system are installed on the Computer PCTUD33. Double click the icon named "Fall-Statischversuch" under

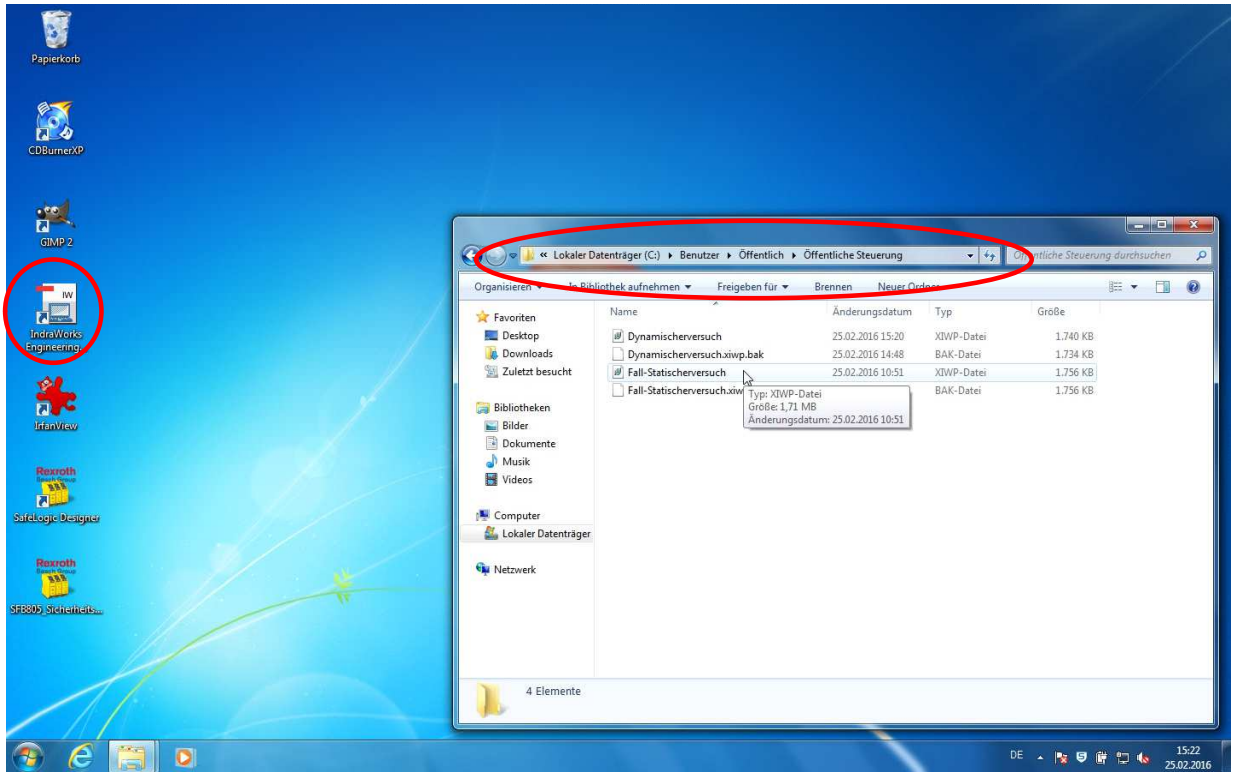

Figure 2.3: NBTUD08: Opening the Indralogic Software program to control the drop tests

the given path `C:\Benutzer\Oeffentlich\OeffentlicheSteurung\Fall-Statischversuch`. This icon can also be found on the desktop of the laptop NBTUD08, refer Fig. 2.3 This is

used to control the operation of the drop tests.

Step 4. From the shortcut menu bar, press B1 to connect the laptop NBTUD08 with the Rexroth controller hardware, see Fig. 2.4. Press B2 to upload the Programmable Logic Control PLC commands from the Laptop on the Rexroth controller hardware.

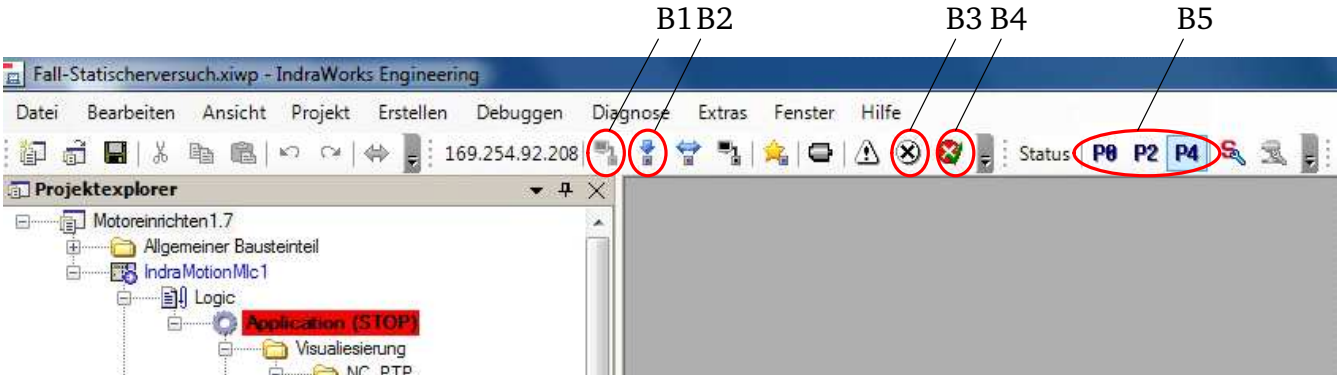

Figure 2.4: Connecting the Laptop with the Controller

If B3 is highlighted as red, click B3 to check the error displayed. The error is displayed if the hardware components of SFB-Demonstrator are not in a stable state. For example, if the door to the housing is left open then the error button B3 is highlighted. Table 2.1 lists the possible error messages. After making the necessary changes, press B4 to clear all the existing error messages

Table 2.1: Possible error descriptions

Error code	Error description	Error solution
F2229216	Keine Leistung Verfügbar	Turn on the blue reset button or check if emergency knobs are activated
F2008027	F8027 Sicher abgeschaltetes Moment bei gesetzt	Close the gate to the housing
F50D2000	Zwangshalt aktiviert	check if emergency buttons are pressed
F2003130	F3130 Fehler beim Überprüfen der Eingangssignale	Close the gate to the housing

from the program. Check B5 if the system is in operational mode P4. Click P4 if the program is in either P0 or P2 state.

Step 5. After setting the program in P4 operational mode, click B6 to login into the IP address of the controller hardware. Select "Ja" in the following prompt message to confirm. Thereafter, select B7 to start the connection between the Indralogic program and the Rexroth controller hardware. Select "Ja" to confirm in the following prompt message.

This can be checked in the following step. Occasionally, the start button B7 is automatically grayed out and the program is in Start mode.

Step 6. To confirm if the IndraLogic program is in start mode, check if B8 displays as "Application (LAUFT)" in green colour. If it displays "Application (STOP)" in red colour, then check

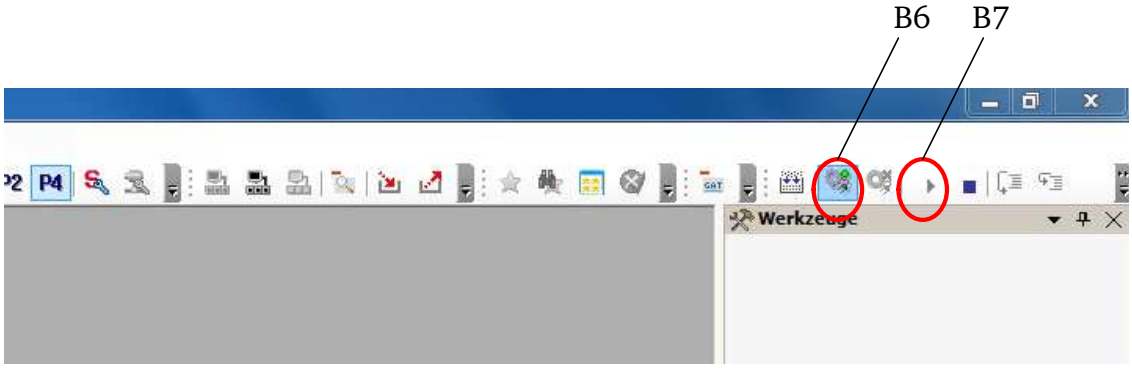

Figure 2.5: Login with the Controller

if the start button B7 is clicked.

Step 7. Open the interface to operate the experimental drop tests of MAFDS by double clicking the "HMI Drive" located at B9 in the Projektexplorer menu on the left side of the Indralogic program. The interface to operate the drop test is illustrated in Fig. 2.6. Check if the tab "Schutz Auslöser freigeshaltet" at B10 is active. It displays green colour if it is activated. In case it is deactivated check if either the emergency buttons or the blue reset button from Fig. 2.1 are deactivated or activated respectively. For the tab "Schutz Auslöser freigeshaltet" at B10 to display green, the blue reset button should be activated and the emergency button deactivated. Proceed to the next step 8. if the tab at B10 displays green.

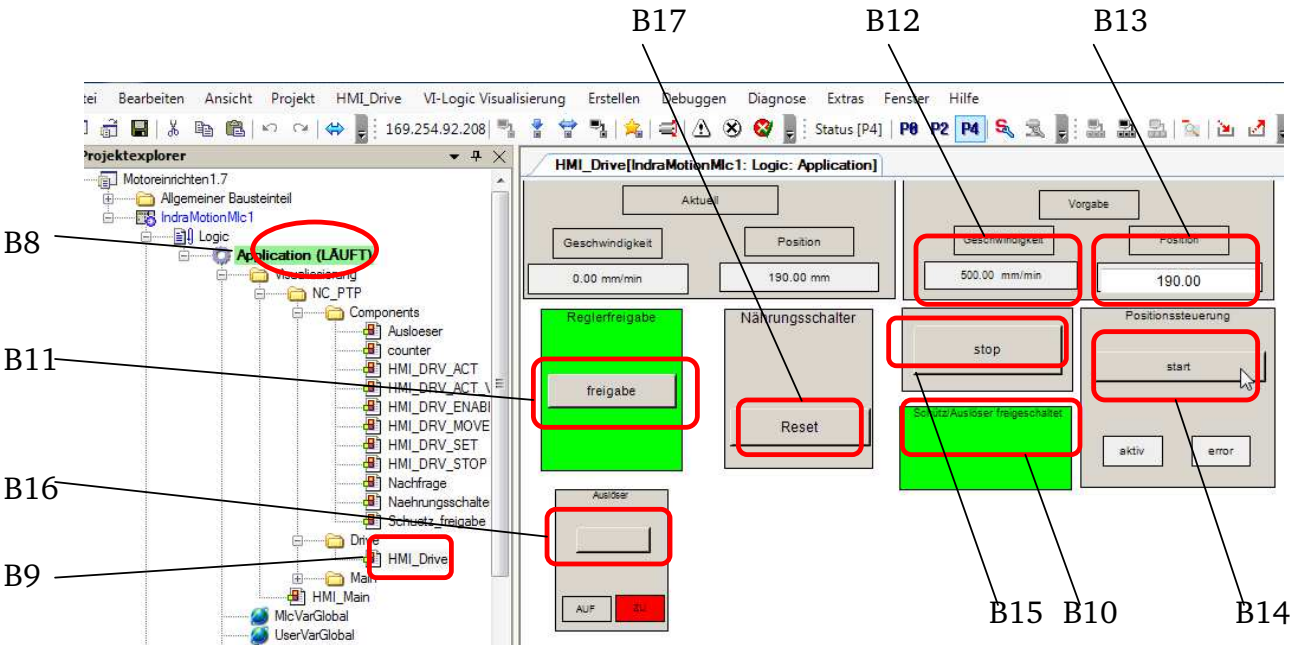

Figure 2.6: Interface to operate the Controller

Step 8. Press B11 to activate the Rexroth controller. It displays green as well once it is activated. It can be activated only if B10 displays green. Ensure there are no errors displayed in B3 from Fig. 2.4. In case of error messages, follow the recommendations listed in table 2.1. Thereafter, press B4 the clear the error messages. It is also important to ensure that the proximity sensor or "Nährungsschalter" in B17 is deactivated. It gets activated if the hoist frame touches the load frame of the MAFDS. Ensure it is in state ps01 before proceeding to step 9, refer table 2.2 for

different states of the proximity sensor.

Step 9. Once the B11 is activated and B17 is deactivated, the experimental drop test can be

Table 2.2: Possible states of the proximity sensor or "Nährungschalter"

Highligted colour	State code	Description
gray	ps01	deactivated by sensor, safe state and parallel movement of MAFDS possible
blue	ps02	activated by sensor, safe state and parallel movement of MAFDS not possible
red	ps03	deactivated manually, dangerous state and parallel movement of MAFDS possible

carried out. The speed in mm/minute of the servomotors to move the MAFDS upwards or downwards can be set from B12. It is recommended not to change the given speed of the servomotors which is 500 mm/min.

Table 2.3: Possible drop heights that can be entered in the Indralogic program

Drop height in m	Position in mm to be entered in B13
0 m	216 mm
0.01 m	206 mm
0.02 m	196 mm
0.039 m	176.1 mm
0.1 m	116 mm
0.216 m	0 mm

Refer Fig. 1.4 for illustration of the servomotor and other components of the SFB 805 demonstrator. For symmetric and non-symmetric drop tests, the position in mm of the MAFDS can be altered from the option B13. For symmetric drop tests, the position when the MAFDS just touches the ground is 216 mm. The maximum drop height can be achieved by entering the position 0 mm. It is to be noted that the maximum drop height $h_{\max} = 0.216$ m and the drop height $h = 0$ m when the MAFDS just touches the ground. Accordingly the various drop heights can be calculated and entered in B13. Be careful while entering the postion in B13, since entering value above 216 mm will lead to forceful compression of MAFDS from the Rexroth controller. Table 2.3 lists some possible drop heights. After entering the required position, press B14 to raise the MAFDS to the required drop height h.

Conversely, it is important to note that the Position to be entered in the "Indralogic program" is different for non-symmetric drop tests. For non-symmetric drop tests, the position when the MAFDS just touches the ground is 192 mm. The table 2.4 lists the possible drop heights that can be entered in the Indralogic program for unsymmetric drop tests. As listed in table 2.4 , the maximum drop height in m for unsymmetric drop test is 0.192 m.

It is to be noted that B12 and B13 input parameters for the speed of servomotors and the position of the hoist frame under the heading "Vorgabe". Similar, parameters can be viewed on the left under the heading "Aktuell". The actual or live values of the speed and the position can be under this heading.

Table 2.4: Possible drop heights that can be entered in the Indralogic program

Drop height in m	Position in mm to be entered in B13
0 m	192 mm
0.01 m	182 mm
0.02 m	172 mm
0.039 m	152.1 mm
0.1 m	92 mm
0.192 m	0 mm

Step 10. After reaching the required drop height h, the servomotors stop automatically and the MAFDS is ready to be dropped. The servomotors can also be prematurely stopped before reaching its final position by pressing the stop button B15. In order to release the MAFDS B16 can be pressed. However, please proceed to the next section before releasing the MAFDS.

2.2 Drop test of MAFDS and recording the measurements

Before releasing the MAFDS make sure the data acquisition DAQ system is turned on. It receives the power from the cabinet controller unit. Referring Fig. 2.2 press the green button to turn on the DAQ system.

Step 11. Turn on the computer PCTUD33 and open double click the software "imc Studio" from the Desktop to manage the DAQ system. The software imc FAMOS Professional 7.1 is utilized to format conversion to MATLAB and conduct statistical analysis of the experimental data. Refer the imc FAMOS manuals for further information.

Step 12. After opening the imc Studio software, click on the previously saved project to record the new experiments. For example, from figure 2.7 select the project named `Kohler_versuche_20170919_v1`". All the sensor and trigger settings are saved from the previous experiments.

Step 13. After opening the previously saved project, select D5 to manage the sensor calibration data, the measurement channels and the trigger settings. As shown in Fig. 2.8, select the tab D1 to view the analog measurement channels that record the experimental output variables of the MAFDS. Click "Kanaltyp: Analoge Eingänge" to view and modify the measurement channels. Select D2 to balance the bridge circuit of the channels for strain gauge sensors. Under D3, all the measurement channels that need to be triggered to record the experimental dynamic output during the drop test of MAFDS can be selected.

The required input information for the measurement channels such as the sensor range, sensitivity, filter settings, sampling frequency and etc. can be managed from D4 console. After making the necessary changes select D6 to start the experiments.

Step 14. Select D7 "Vorbereiten" to configure the imc Studio program with the DAQ hardware systems. After the software is connected and configured with the hardware DAQ system,

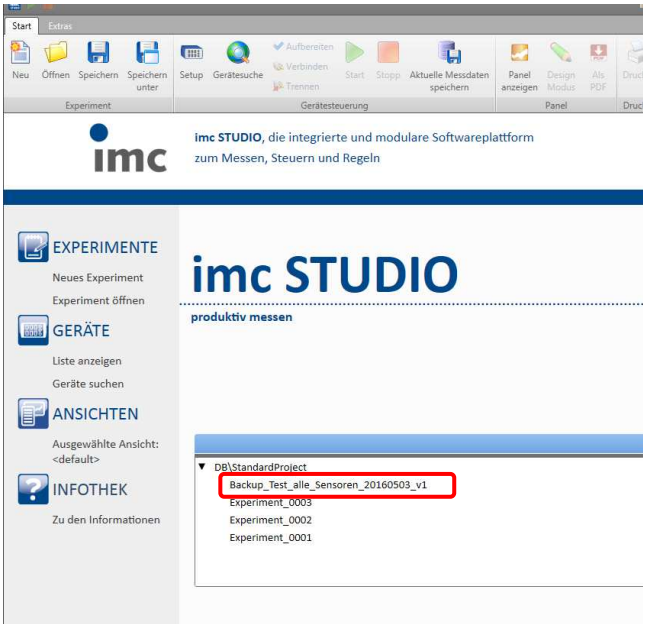

Figure 2.7: Opening the previous experiment set up

press D8 "Start" to start the experiments. Once the MAFDS is released, the cabinet controller sends a trigger signal to the hardware DAQ system and the experimental recording begins.

To release the MAFDS from the drop height h, refer Fig. 2.9. Press the tab "Auslöser" to release the MAFDS from the hoist frame. Next, select the option "Ja" to confirm the release of MAFDS. After selecting "Ja", a countdown of 5 seconds begins after which the MAFDS is released. Moreover, the digital signal from the cabinet controller triggers the recording of the measured output variables of MAFDS. This can be noticed from the plots on the interface of imc Studio Software. After the buffer time of 5 seconds, the MAFDS is released by a electrical-pneumatic coupling mechanism.

The dynamic behaviour is evident from the plots of measured ouputs in Fig. 2.10. The recording of the measured output variables can be viewed by dragging the variable names seen on the right hand side of the interface on the gray field area.

Step 15. After recording the drop test experimental results, the data can be saved in Matlab format for further analysis using the imc FAMOS Professional 7.1 software. For saving the data in MATLAB format, open the imc FAMOS Professional 7.1 software from the desktop of PCTUD33. Open the path `C:/Users/Public/Documents/DB/StandardProject/Kohler_versuche_20170919_v1`" from the explorer. Open the folder which is named automatically after the current time and date (above "Config") to view the saved measured output variables. Right click to load any of the variables. Use the save option on the left hand side of the imc FAMOS interface to save the loaded variable as a MATLAB file.

2.3 Recoupling MAFDS with the hoist frame

Step 16. The final step is to recouple the released MAFDS with the hoist frame. Enter position as an arbitrary value of around 290 mm. As soon as the hoist frame meets the load frame of MAFDS, the proximity sensor gets activated to blue colour.

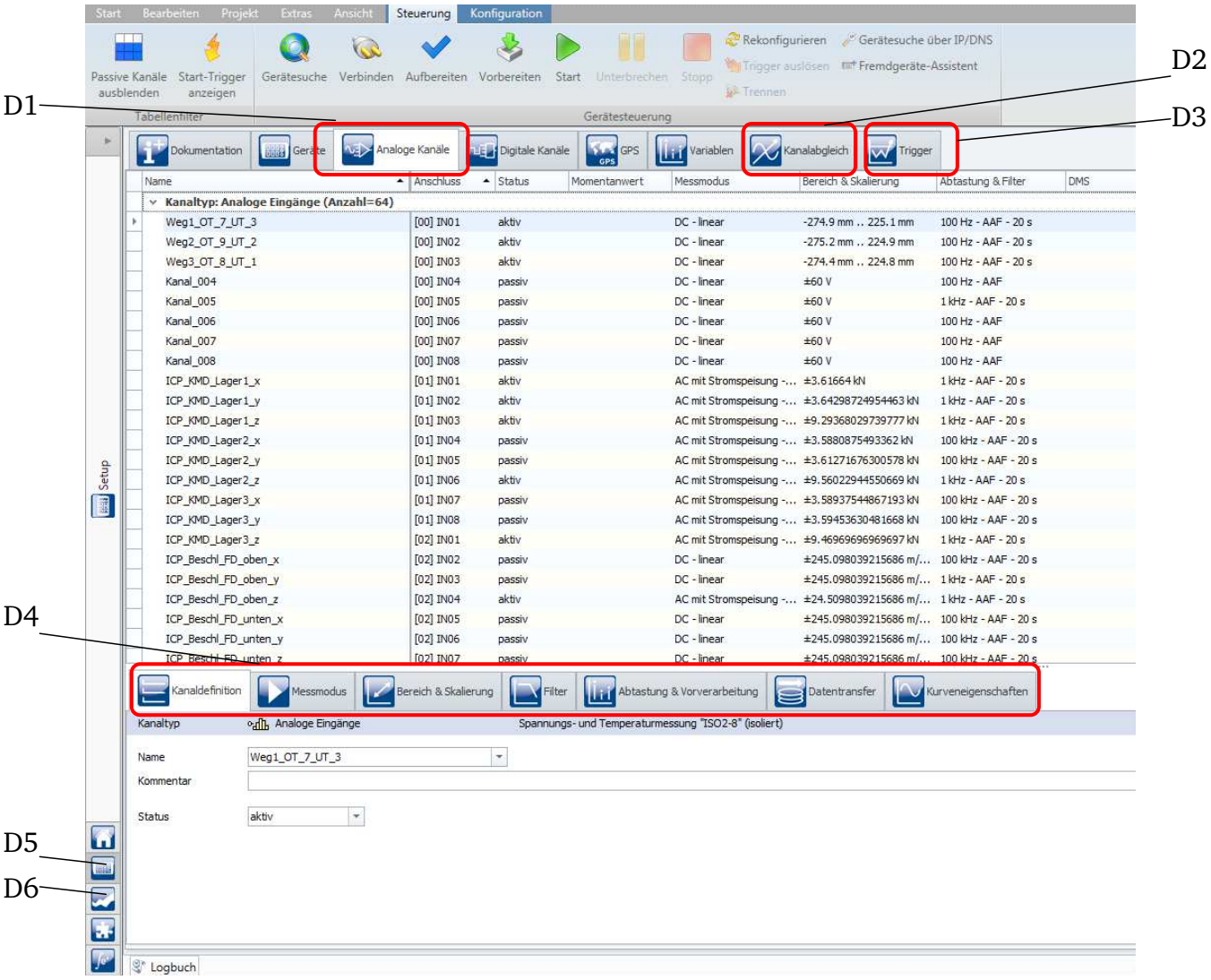

Figure 2.8: Interface to manage the sensor and trigger settings

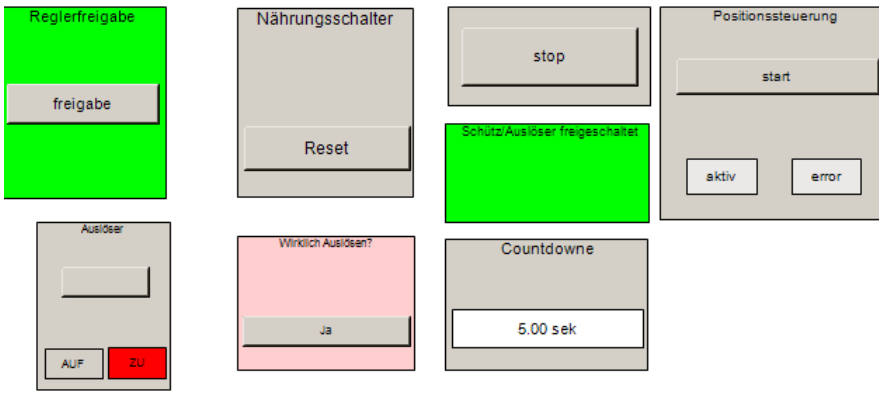

Figure 2.9: Release mechanism of MAFDS

After the proximity sensor is activated, deactivate it manually by clicking "Nährungsschalter". Thereafter, the display turns red in colour. Next, click "Auflöser" to recouple the MAFDS with the hoist frame. Notice that the highlighted display changes from "AUF" to "ZU", refer Fig. 2.13.

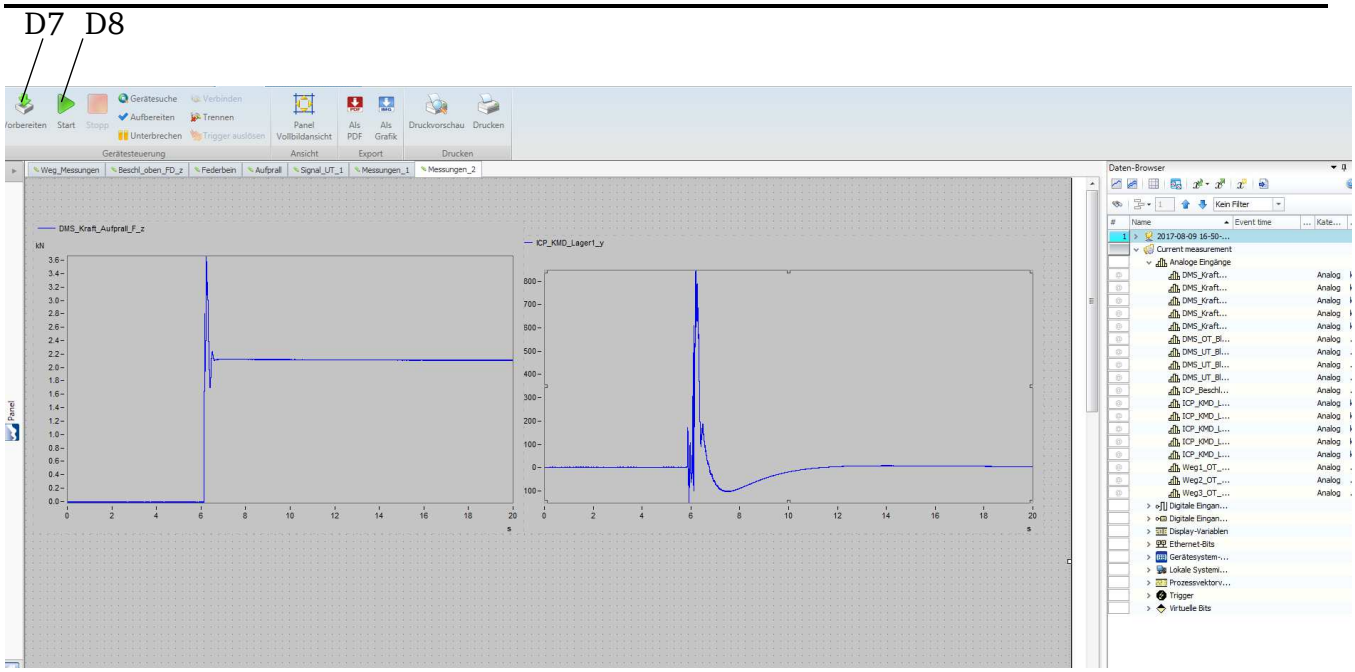

Figure 2.10: Activate the DAQ to record experiments

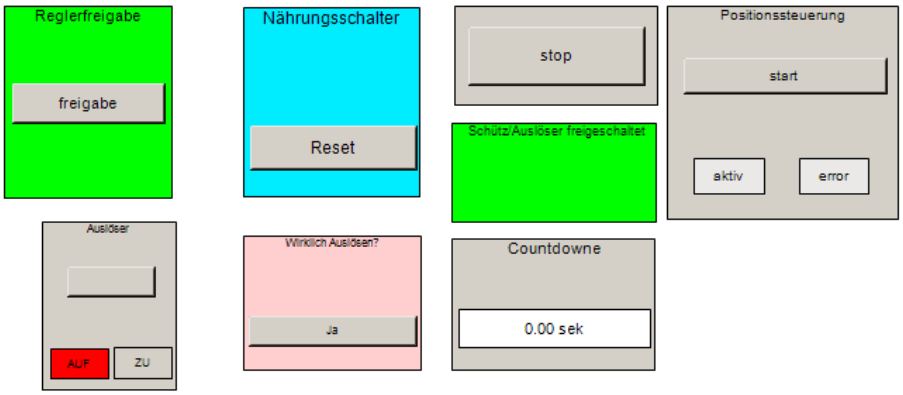

Figure 2.11: Activation of proximity sensor

Step 17. After coupling the MAFDS, the MAFDS can be driven to a new drop height by entering the required position in mm. One should be careful while entering the position values. Don't enter the value greater than the present position as it may further compress the MAFDS forcefully leading to possible structural damage to its components.

Step 18. After reaching the final position, press the proximity sensor to reset its functionality. Notice the change in colour from red to gray, refer Fig. 2.13.

Step 19. PCTUD33: Save the experiments in imc Studio and close the program. Click "Yes" to the prompt message for saving the changes made to the experiment.

Step 20. NBTUD08: Click B11 from Fig. 2.6 to deactivate the controller. Press the stop button on the right side of option B7. Next, click the logout button on the right of option B6. Click "Ok or Ja" for all the following prompt messages.

In the end, close the program and click "Ja" to both the following prompt messages.

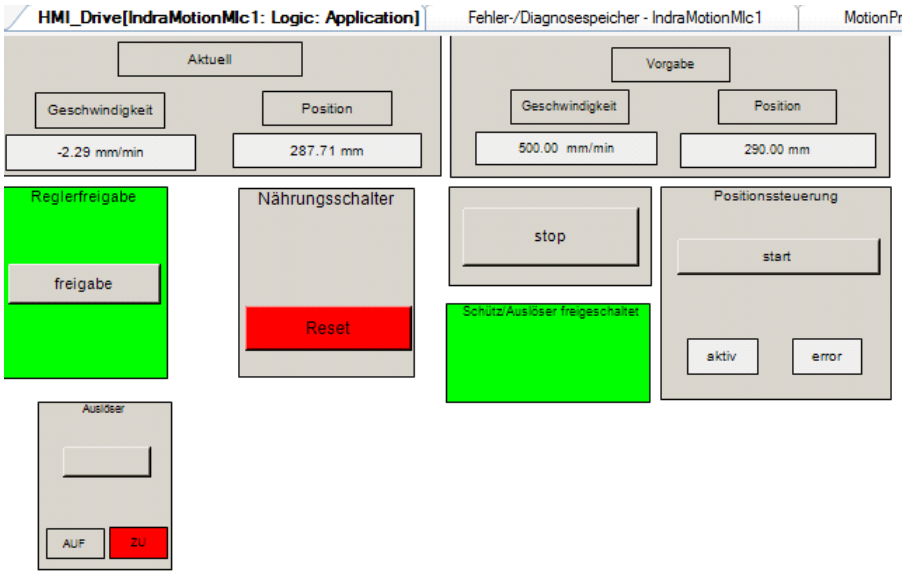

Figure 2.12: Deactivate the proximity sensor and move the MAFDS in the upward direction

Figure 2.13: The final state of the interface of Indralogic program

3 Simulation models

To predict the dynamic behavior of the MAFDS, two types of numerical simulation models are utilized. The first one is a simple two degree freedom mass spring damper system and the second one is a finite element model.

3.1 Two mass spring damper

Fig. 3.1 shows a simplified two degree of freedom (2DOF) mathematical model of the MAFDS. It is utilized to predict the global dynamic output of the spring damper component and the ground impact force of MAFDS under varying drop heights and payloads. The internal loads in the upper and lower trusses are neglected. The upper and lower structures of the MAFDS are simplified as two lumped upper mass m_u and lower mass m_l. The spring-damper component is represented by the stiffness parameter k and the viscous damping coefficient b. Similarly, the elastic foot is represented by the stiffness parameter k_{ef}. The 2DOF mathematical model has two degrees of freedom that are defined by the local translational displacements z_u and z_l.

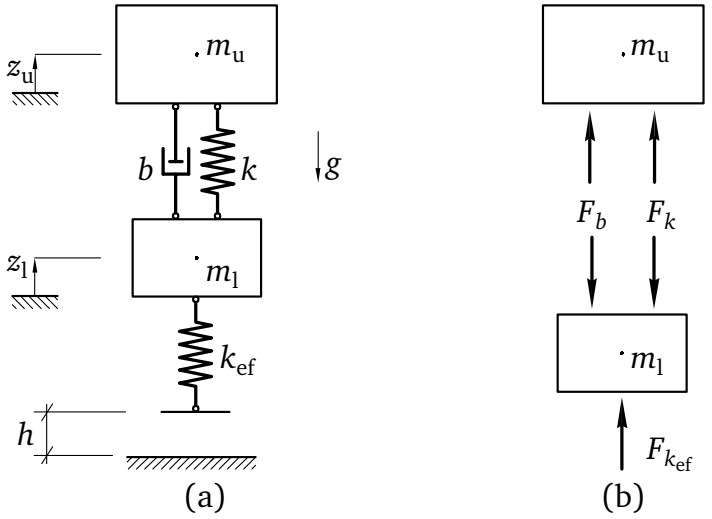

Figure 3.1: Illustration of simplified 2DOF mathematical model of MAFDS: a) principal sketch and b) internal free forces

The goal is to predict the maximum dynamic response vector

$$\boldsymbol{y}_m = \begin{bmatrix} z_{r,max} \\ F_{sd,max} \\ F_{ef,max} \end{bmatrix} = \max \begin{bmatrix} z_u - z_l \\ k\,(z_u - z_l) + b\,(\dot{z}_u - \dot{z}_l) \\ k_{ef}\, z_l \end{bmatrix} \tag{3.1}$$

that is related to the displacements z_u, z_l and the velocities $\dot{z}_u$, $\dot{z}_l$. It consists of the maximum compression $z_{r,max}$, maximum spring-damper force $F_{sd,max}$ and the maximum ground impact force $F_{ef,max}$.

In this mathematical model, the stiffness $k(z_r)$ of the spring is not constant and is modelled as a function that is dependent upon the value of the relative displacement $z_r = (z_u - z_l)$. Similarly,

the non-linear viscous damping $b(\dot{z}_\mathrm{r})$ is dependent on the relative velocity $\dot{z}_\mathrm{r}$. This is further illustrated in [7] and [8].

The matrix form of the homogeneous governing differential equation is

$$\underbrace{\begin{bmatrix} m_\mathrm{u} & 0 \\ 0 & m_\mathrm{l} \end{bmatrix}}_{\boldsymbol{M}} \begin{pmatrix} \ddot{z}_\mathrm{u} \\ \ddot{z}_\mathrm{l} \end{pmatrix} + \underbrace{\begin{bmatrix} b(\dot{z}_\mathrm{r}) & -b(\dot{z}_\mathrm{r}) \\ -b(\dot{z}_\mathrm{r}) & b(\dot{z}_\mathrm{r}) \end{bmatrix}}_{\boldsymbol{B}(\dot{z}_\mathrm{r})} \begin{pmatrix} \dot{z}_\mathrm{u} \\ \dot{z}_\mathrm{l} \end{pmatrix} + \underbrace{\begin{bmatrix} k(z_\mathrm{r}) & -k(z_\mathrm{r}) \\ -k(z_\mathrm{r}) & k(z_\mathrm{r}) + k_\mathrm{ef} \end{bmatrix}}_{\boldsymbol{K}(z_\mathrm{r})} \begin{pmatrix} z_\mathrm{u} \\ z_\mathrm{l} \end{pmatrix} = \begin{pmatrix} 0 \\ 0 \end{pmatrix}. \tag{3.2}$$

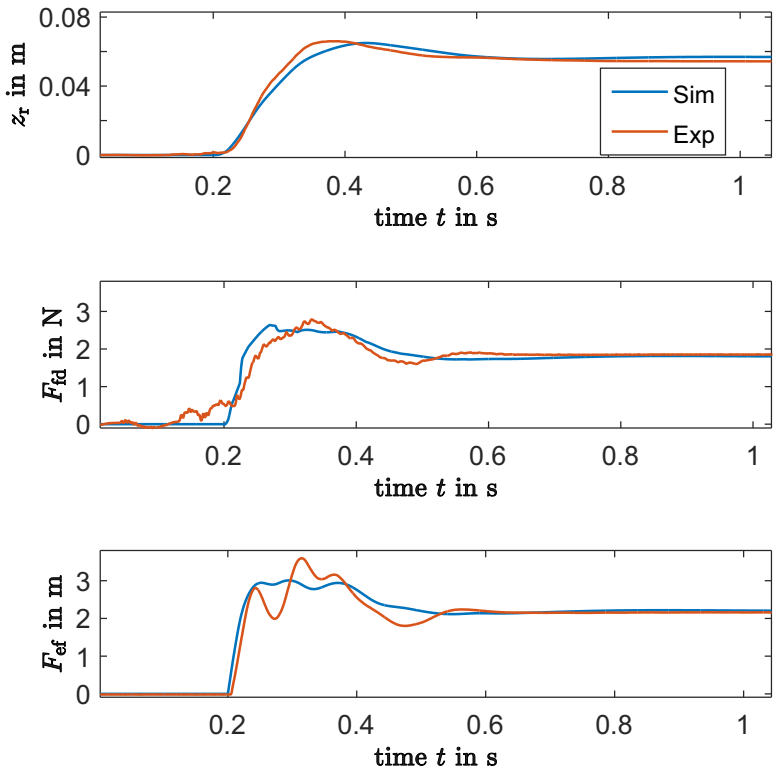

Figure 3.2: Comparison of experimental results and simulation results of a 2 mass spring damper model of drop test with $h = 0.1$ m

The two mass spring damper simulation model of MAFDS is saved under the path: `0:\Arbeitsgruppen\SFB805\SFB_Demonstrator\2_Simulation\01_MAFDS_Zweimassenschwinger_Matlab_Simulink`

3.2 Finite element model

As illustrated in Fig. 3.3, the multi degree of freedom (MDOF) finite element (FE) model consists of the upper truss, the lower truss, kinematic guidance links, spring-damper component and the elastic foot. The structure is modelled using the commercial FE software ANSYS Classic. The upper and lower truss comprises of beam-columns with the same length $l_{\mathrm{bc}} = 0.45$ m , Young's modulus $E_{\mathrm{bc}} = 71.7 \cdot 10^9$ N m^{-2} and density $\rho_{\mathrm{bc}} = 2810$ kg m^{-3} that are modelled with the Beam189 element. This three-node beam element is based on TIMOSHENKO beam theory which includes shear-deformation effects and the corresponding nodes have three translational and three rotational DOF in and about $x-$, $y-$ and $z-$ directions. In the FE model, the beam-columns are connected with each other by a rigid constraint beam element MPC184, thereby allowing bending moments in the deformable beam-columns. Similarly, the kinematic guidance

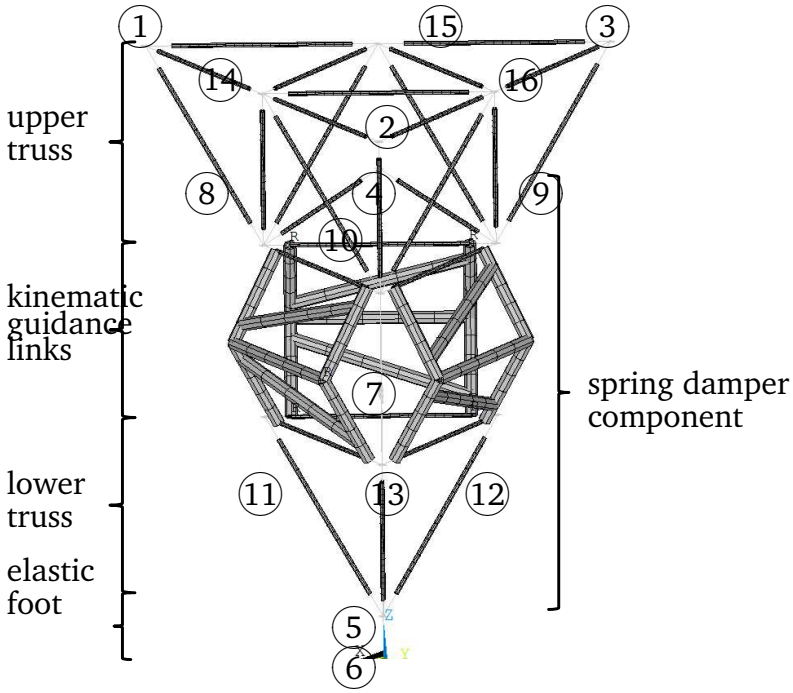

Figure 3.3: finite element model

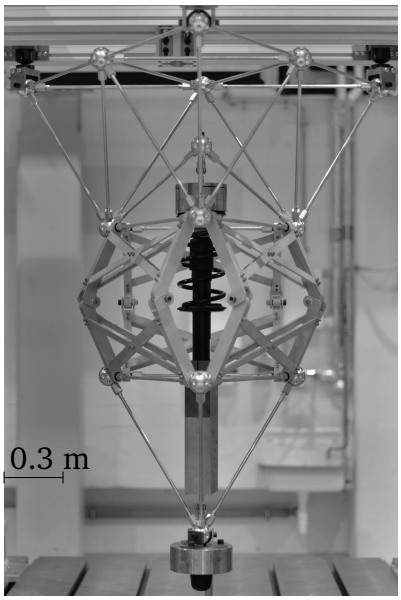

Figure 3.4: photo of experimental prototype

links are represented by elastic Beam189 element with Young's modulus $E_{\mathrm{gl}} = 71.7 \cdot 10^9$ N m^{-2} and density $\rho_{\mathrm{gl}} = 2810$ kg m^{-3} and the kinetic movement of the guidance links is enabled by the frictionless MPC184 revolute joints. The nonlinear spring behaviour is implemented using COMBIN39 element, where the stiffness depends nonlinearly upon the relative compression in the vertical $z-$ direction of the spring-damper. The nonlinear damping is modelled using a nonlinear joint element MPC184, where the viscous damping coefficient is dependent upon the relative velocity of the spring-damper component. The elastic foot of MAFDS is represented by MATRIX27 element, which consists of stiffness terms in the $x-$, $y-$ and $z-$ lateral directions.

Tab. 3.1 lists the summary of output variables predicted by the FE model that is validated by the experimentally obtained outputs. The location numbers in Tab. 3.1 correspond to the encircled numbers in Fig. 3.3. As shown in Fig. 3.4, the experimental output data is obtained from the test rig of MAFDS.

Table 3.1: Summary of output variables

Output variable	Output location	Location Nr.
Force	support to housing frame, spring-damper, elastic foot	1-6
Acceleration	spring-damper component, elastic foot	4-5
Compression	vertical displacement between upper and lower truss	7
Axial load	beam columns in upper and lower trusses	8-13
Bending Moment	beam columns in upper and lower trusses	8-16

Figure 3.5 illustrates the comparison between some of the measured and the simulated output variables that are predicted using a non-linear finite element model. The FE simulation and the experiment was conducted for a symmetric drop test scenario with a given drop height $h = 0.05$ m and mass of MAFDS as 225 kg.

The FE model of MAFDS is saved under the path: `O:\Arbeitsgruppen\SFB805\SFB_Demonstrator\2_Simulation\02_FE_Ansys_Modell_Goe_Mal`

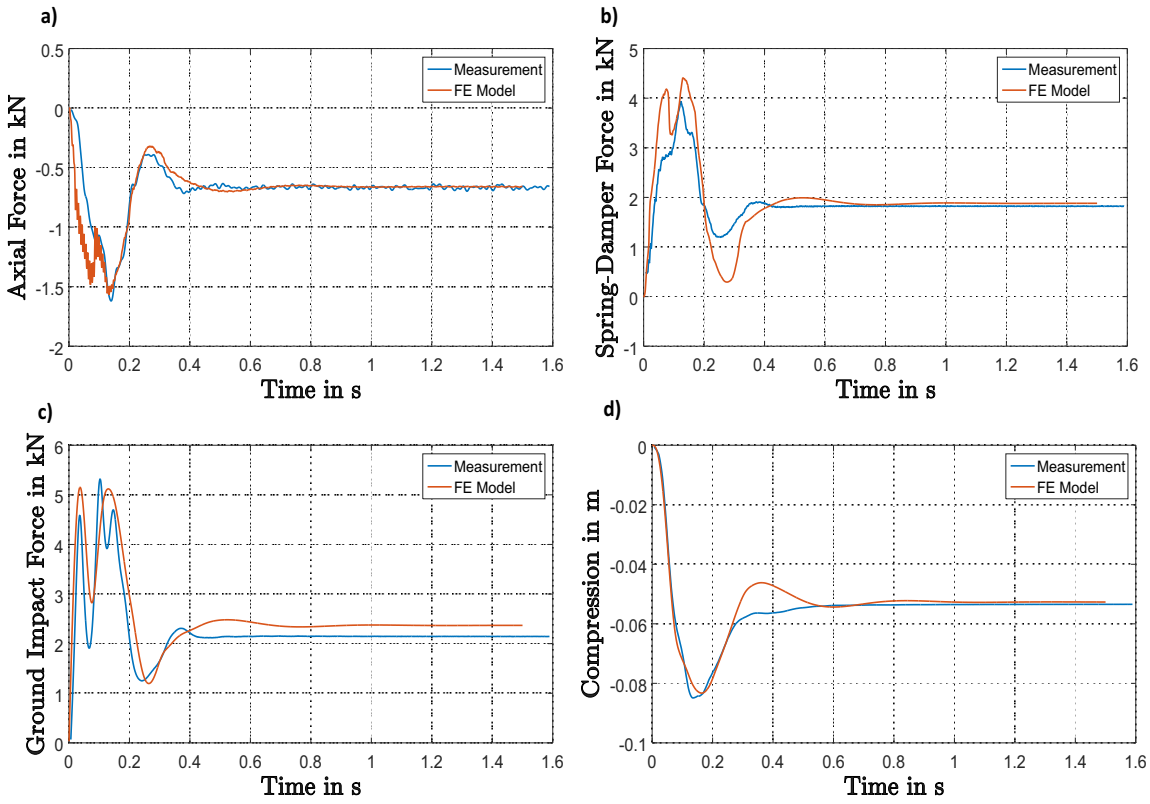

Figure 3.5: Comparison of measured and FE simulated output variables: a) axial load at 8, b) spring-damper force at 4, c) ground impact force at 6, and d) compression at 7

4 Measurement results of MAFDS

The measurements on the experimental prototype MAFDS were conducted primarily to validate the 2-mass-spring damper and the FE simulation models under static as well as symmetric and unsymmetric drop tests. A brief description about the static as well as the symmetric and unsymmetric drop tests is described in the chapter 1. Till date, the objectives of conducting the experimental tests on the MAFDS can be summarized as:

1. **Estimation of the non-linear characteristics of the spring-damper component of the MAFDS**. As seen in Fig. 4.1, the non-linear spring stiffness behaviour is estimated by static loading of MAFDS, whereas the non-linear damping is estimated by conducting the symmetric drop tests. Further details of the tests are described in [7] and [8].

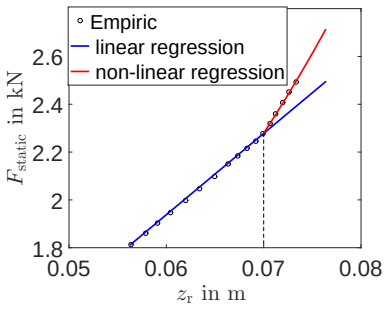

Figure 4.1: Stiffness curve

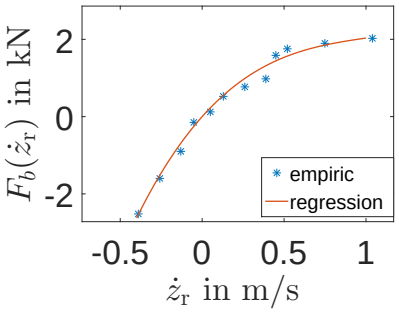

Figure 4.2: Damping curve

The experimental data as well as the MATLAB codes for the experiments can be found under: `O:\Arbeitsgruppen\SFB805\SFB_Demonstrator\5_Messungen\MAFDSMessungen\01_exp_stiffness_damp`

2. **Model validation of simulation models of MAFDS**
   For model validation, the experimental drop tests are designed using a simple full factorial (FF) design by varying the mass of the upper structure $m_{\text{u,e}}$ and the drop height h_{e} of the experimental MAFDS, [9]. The FF design takes into account the combinations within a certain range and amount of tests of independent variables and the order of experimental test of these combinations are randomized to avoid systematic errors. In this approach, the significance of the two independent variables $m_{\text{u,e}}$ and h_{e}, each having three different values is considered, see Tab. 4.1.

   Fig. 4.3 shows the 3x3 FF design of experiments using $m_{\text{u,e}}$ and h_{e} as varying input variables. This design takes into account both the main effects and the interaction effects of the

Table 4.1: FF design of experiments with experimental upper mass $m_{\text{u,e}}$ and the experimental drop height h_{e}

Variable level	Mass variable $m_{\text{u,e}}$	Value in kg	Drop height variable h_{e}	Value in m
1	$m_{\text{u,e,1}}$	185	$h_{\text{e,1}}$	0.03
2	$m_{\text{u,e,2}}$	205	$h_{\text{e,2}}$	0.04
3	$m_{\text{u,e,3}}$	225	$h_{\text{e,3}}$	0.05

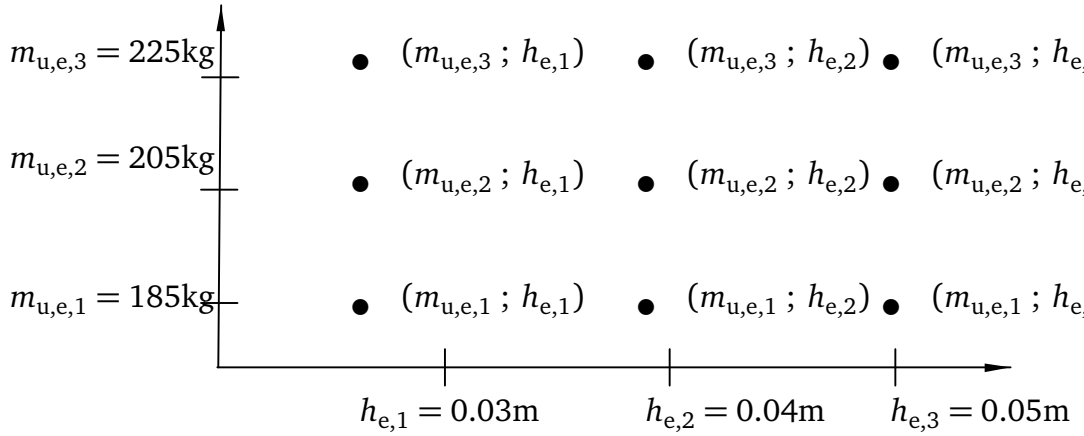

Figure 4.3: 3^2 FF design of experiments on MAFDS

two variables $m_{u,e}$ and h_e. The main effect considers the influence of one independent variable on the output vector $\boldsymbol{y}_e$, while ignoring the influence of other independent variables. In Fig. 4.3, the experimental mass $m_{u,e}$ varies as per the combinations of $(m_{u,e,1}\ ;\ h_{e,1})$, $(m_{u,e,2}\ ;\ h_{e,1})$ and $(m_{u,e,3}\ ;\ h_{e,1})$, while the experimental drop height h_e remains constant. In this case, the variation in the experimental output $\boldsymbol{y}_e$ is influenced by single variable $m_{u,e}$. Conversely, an interaction effect of the independent variable occurs when its influence on the output relies on the value of the other independent variable also. For example, in the combinations $(m_{u,e,2}\ ;\ h_{e,3})$ and $(m_{u,e,3}\ ;\ h_{e,2})$ the output $\boldsymbol{y}_e$ is influenced by both $m_{u,e}$ and h_e.

The measured output variables for the 3x3 factorial tests are saved under the path `0:\Arbeitsgruppen\SFB805\SFB_Demonstrator\5_Messungen\MAFDSMessungen\01_exp_stiffness_damp`

3. **Symmetric and non-symmetric drop tests**

Moreover, experimental drop tests were conducted on the MAFDS to analyse its dynamic

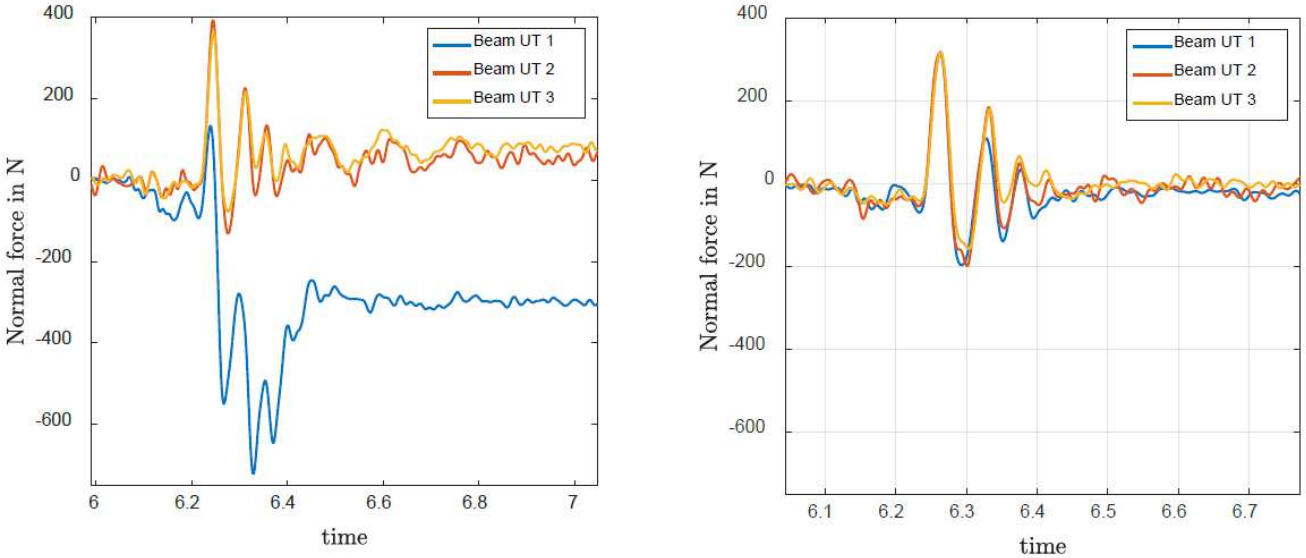

a) non-symmetric drop test b) symmetric drop test

Figure 4.4: Comparison of normal force in the beam columns of lower truss

behaviour with symmetric as well as non-symmetric inclination. Non-symmetic inclination

of MAFDS is achieved by placing additional displacement blocks in the housing support of the MAFDS. For instance, Fig. 4.4 depicts the comparison between the normal load distribution in the beam-columns of MAFDS under symmetric and non-symmetric drop tests with a drop height $h = 0.07$ m. In the case of Fig. 4.4 b), the normal load is equally distributed only in the two beam columns of the lower truss. Conversely, in the case of Fig. 4.4 a), it is seen that all the three beam-columns of the lower truss are subjected to equally distributed normal forces.

The experimental data for the measured output variables that are recorded for different drop heights $h_e = 0.1, 0.2, ..., 0.7$ m with symmetric as well as non-symmetric inclination is saved under: `0:\Arbeitsgruppen\SFB805\SFB_Demonstrator\5_Messungen\MAFDSMessungen\03_Smmetric_and_Non_symmetric_drop_tests`.

4. **Experiments for a Journal Paper by Prof. Kohler**
   Under collaboration with Prof. Kohler, 100 normally distributed experimental drop tests

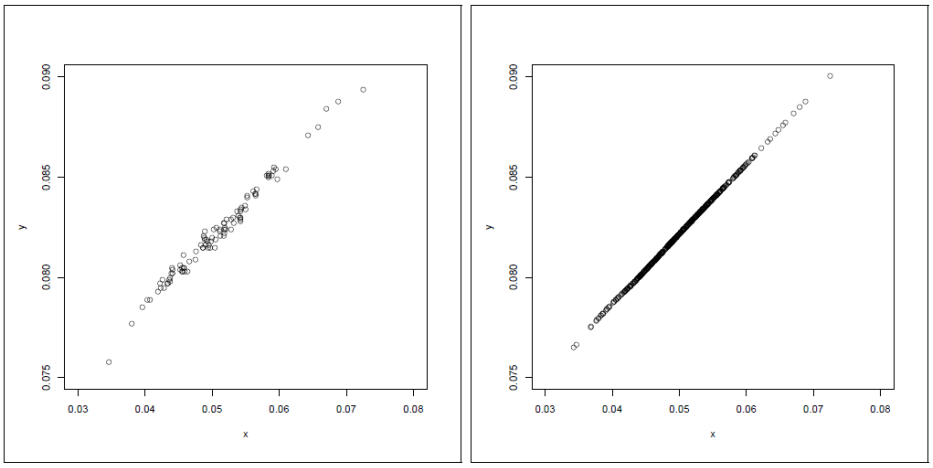

Figure 4.5: Relative compression of spring-damper componenent due to normally distributed experimental drop tests of MAFDS, [10]

of MAFDS were conducted to compare the observed relative compression of the spring-damper component with the simulation results of a 2 mass spring damper system. The experimenatal as well as simulation data is saved under the path: `0:\Arbeitsgruppen\SFB805\SFB_Demonstrator\5_Messungen\MAFDSMessungen\04_Kohler_experiments`.

Figure 4.6 depicts the location of the sensors that measure the experimental output variables of the MAFDS. Tab. 4.2 and Tab. 4.3 list all the measurement channels that are connected to the data acquisition system DAQ of the MAFDS. The DAQ is described in section 2.2.

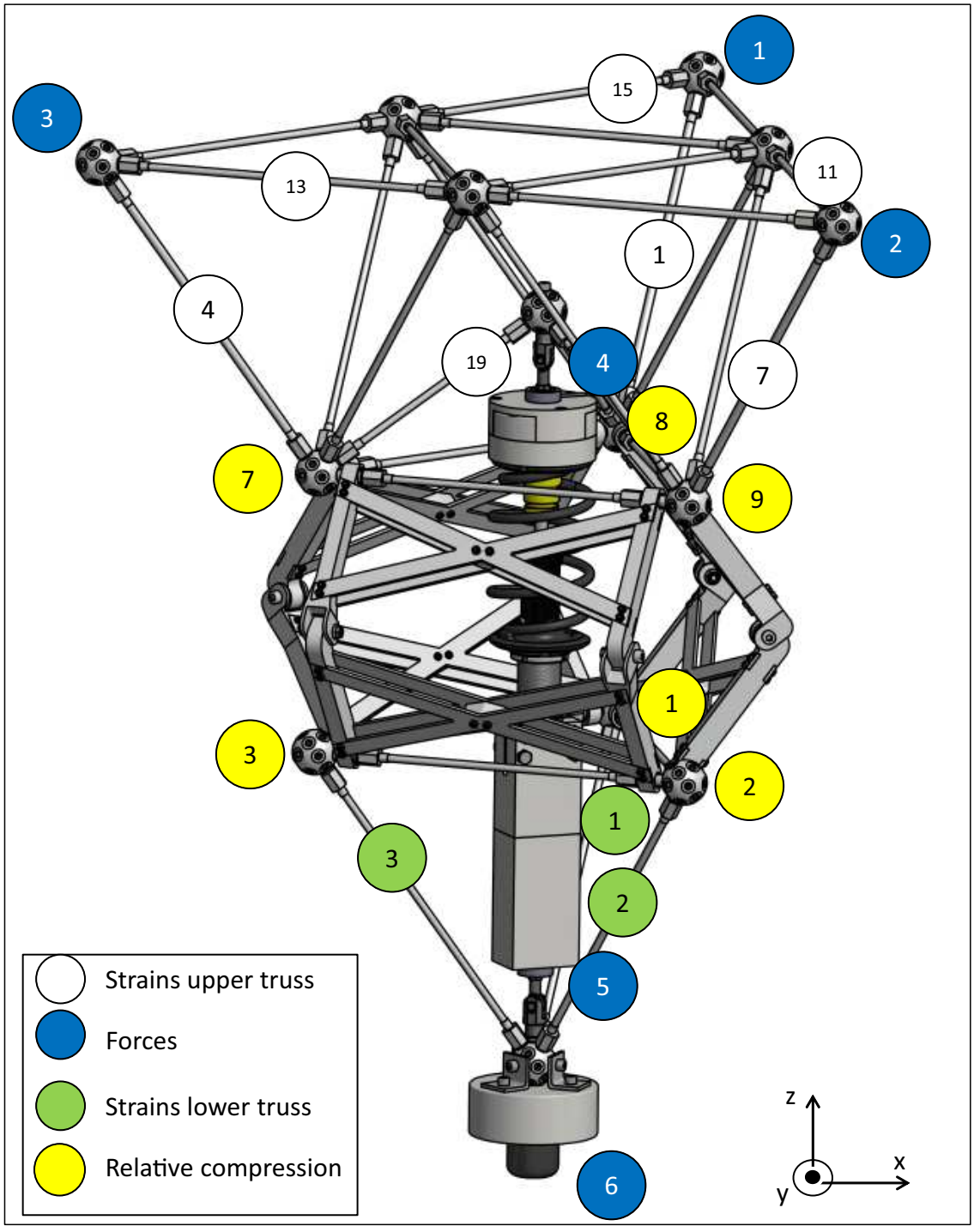

Figure 4.6: Location of sensors in MAFDS

Table 4.2: Summary of experimental output channels

Output channel	Location	Output	SI	Direction
ICP_KMD_Lager1_x	1	housing support force	kN	global x
ICP_KMD_Lager1_y	1	housing support force	kN	global z
ICP_KMD_Lager1_z	1	housing support force	kN	global y
ICP_KMD_Lager2_x	2	housing support force	kN	global x
ICP_KMD_Lager2_y	2	housing support force	kN	global z
ICP_KMD_Lager2_z	2	housing support force	kN	global y
ICP_KMD_Lager3_x	3	housing support force	kN	global x
ICP_KMD_Lager3_y	3	housing support force	kN	global z
ICP_KMD_Lager3_z	3	housing support force	kN	global y
DMS_Kraft_OT_kn_10	4	spring damper force above	kN	global z
DMS_Kraft_UT_kn_4	5	spring damper force below	kN	global z
DMS_Kraft_Aufprall_F_x	6	ground impact force	N	global x
DMS_Kraft_Aufprall_F_y	6	ground impact force	N	global y
DMS_Kraft_Aufprall_F_z	6	ground impact force	N	global z
DMS_OT_Bl_1_z_plus	1	normal strain		local positive x
DMS_OT_Bl_1_z_minus	1	normal strain		local negative x
DMS_OT_Bl_1_by	1	bending strain		local y
DMS_OT_Bl_4_z_plus	4	normal strain		local positive x
DMS_OT_Bl_4_z_minus	4	normal strain		local negative x
DMS_OT_Bl_4_by	4	bending strain		local y
DMS_OT_Bl_7_z_plus	7	normal strain		local positive x
DMS_OT_Bl_7_z_minus	7	normal strain		local negative x
DMS_OT_Bl_7_by	7	bending strain		local y
DMS_OT_Bl_19_z_plus	19	normal strain		local positive x
DMS_OT_Bl_19_z_minus	19	normal strain		local negative x
DMS_OT_Bl_19_by	19	bending strain		local y
DMS_OT_Bl_11_by	11	bending strain		local y
DMS_OT_Bl_11_bz	11	bending strain		local z
DMS_OT_Bl_13_by	13	bending strain		local y
DMS_OT_Bl_13_bz	13	bending strain		local z
DMS_OT_Bl_15_by	15	bending strain		local y
DMS_OT_Bl_15_bz	15	bending strain		local z
DMS_UT_Bl_1_z_plus	1	normal strain		local positive x
DMS_UT_Bl_1_z_minus	1	normal strain		local negative x
DMS_UT_Bl_1_by	1	bending strain		local y

Table 4.3: Summary of experimental output channels

Output channel	Location	Output	SI	Direction
DMS_UT_Bl_2_z_plus	2	normal strain		local positive x
DMS_UT_Bl_2_z_minus	2	normal strain		local negative x
DMS_UT_Bl_2_by	2	bending strain		local y
DMS_UT_Bl_3_z_plus	3	normal strain		local positive x
DMS_UT_Bl_3_z_minus	3	normal strain		local negative x
DMS_UT_Bl_3_by	3	bending strain		local y
Weg1_OT_7_UT_3	7 & 3	relative compression		local y
Weg2_OT_9_UT_2	9 & 2	relative compression		local y
Weg3_OT_8_UT_1	8 & 1	relative compression		local y

Bibliography

[1] Enss, G., Gehb, C., Götz, B.; Melz, T., Ondoua, S., Platz, R., Schäffner, M., Load transferring device, Patent DE102014106858.A1, 2015.

[2] Schäffner. M et al., "Entwicklung des SFB-Demonstrators", Technische Universität Darmstadt, 2016

[3] Schaeffner, M., Goetz, B., Platz, R., "Active buckling control of a beam-column with circular cross-section using piezoelastic supports and integral LQR control", Journal of Smart Materials and Structures, 2016.

[4] Gehb, C.,Platz, R., Melz, T., "Active load path adaption in a simple kinematic load-bearing structure due to stiffness change in the structure supports", Journal of Physics, Conference Series 744, 2016.

[5] Goetz, B., Schaeffner, M., Platz, R., Melz, T.: "Lateral vibration attenuation of a beam with circular cross-section by a support with integrated piezoelectric transducers shunted to negative capacitances", Journal of Smart Materials and Structures, 2016.

[6] Enss, G., Platz, R., "Evaluation of uncertainty in experimental active buckling control of a slender beam-column using Weibull analysis", Journal of Mechanical Systems and Signal Processing, 2016.

[7] Mallapur, S., Platz, R.: "Quantification and Evaluation of Uncertainty in the Mathematical Modelling of a Suspension Strut using Bayesian Model Validation Approach", In: Proceedings of Conference IMAC-XXXV, Garden Grove, California, USA, 2017

[8] Mallapur, S., Platz, R.: "Bayesian Inference Approach to evaluate the uncertainty in the Mathematical Modelling of a Suspension Strut", Accepted: Conference ICEDyn 2017, Ericeira, Portugal, 2017

[9] Dean, A., Voss, D. "Design and Analysis of Experiments", Springer Verlag New York, 1999

[10] Kohler, M., Krzyzak, A., Mallapur, S., Platz, R.,"Uncertainty Quantification in case of Imperfect Models: A Non-Bayesian Approach", Submitted: Scandinavian Journal of Statistics, 2017